OPEN ACCESS

Clinical science

Detection of diabetic neovascularisation using single-capture 65°-widefield optical coherence tomography angiography

Heiko Stino ,[1] Michael Niederleithner,[2] Johannes Iby ,[1] Aleksandra Sedova,[1] Thomas Schlegl,[2] Irene Steiner,[3] Stefan Sacu,[1] Wolfgang Drexler,[2] Tilman Schmoll,[2,4] Rainer Leitgeb,[2] Ursula Margarethe Schmidt-Erfurth ,[1] Andreas Pollreisz [1]

[1]Department of Ophthalmology, Medical University of Vienna, Vienna, Austria
[2]Center for Medical Physics and Biomedical Engineering, Medical University of Vienna, Vienna, Austria
[3]Center for Medical Statistics, Informatics and Intelligent Systems, Section for Medical Statistics, Medical University of Vienna, Vienna, Austria
[4]Carl Zeiss Meditec Inc, Dublin, California, USA

Correspondence to
Dr Andreas Pollreisz, Department of Ophthalmology, Medical University of Vienna, Wien, 1090, Austria; andreas.pollreisz@meduniwien.ac.at

Received 1 July 2022
Accepted 26 October 2022
Published Online First 14 November 2022

To cite: Stino H, Niederleithner M, Iby J, *et al*. *Br J Ophthalmol* 2024;**108**:91–97.

ABSTRACT

Aim To assess the detection rate of retinal neovascularisation (NV) in eyes with proliferative diabetic retinopathy (PDR) using widefield optical coherence tomography angiography (WF-OCTA) in comparison to ultrawidefield fluorescein angiography (UWF-FA).

Methods Single-capture 65°-WF-OCTA-imaging was performed in patients with NV at the disc or elsewhere (NVE) detected on UWF-FA using a modified PlexElite system and B-scans were examined for blood flow signals breaching the internal limiting membrane. Sensitivity of WF-OCTA and UWF colour fundus (UWF-CF) photography for correct diagnosis of PDR was determined and interdevice agreement (Fleiss' κ) between WF-OCTA and UWF-FA for detection of NV in the total gradable area and each retinal quadrant was evaluated.

Results Fifty-nine eyes of 41 patients with PDR detected on UWF-FA were included. Sensitivity of detecting PDR on WF-OCTA scans was 0.95 in contrast to 0.78 on UWF-CF images. Agreement in detecting NVE between WF-OCTA and UWF-FA was high in the superotemporal (κ=0.98) and inferotemporal (κ=0.94) and weak in the superonasal (κ=0.24) and inferonasal quadrants (κ=0.42). On UWF-FA, 63% of NVEs (n=153) were located in the temporal quadrants with 93% (n=142) of them being detected on WF-OCTA scans.

Conclusion The high reliability of non-invasive WF-OCTA imaging in detecting PDR can improve clinical examination with the potential to replace FA as a single diagnostic tool.

WHAT IS ALREADY KNOWN ON THIS TOPIC

⇒ Optical coherence tomography angiography (OCTA) allows non-invasive detection of diabetic neovascularisation (NV). A large field of view is often required for correct diagnosis of proliferative diabetic retinopathy (PDR) and is commonly achieved in commercially available systems by montaging of several scans, which takes time and patient compliance.

WHAT THIS STUDY ADDS

⇒ This study is the first to evaluate sensitivity of PDR diagnosis and NV detection using a single-capture 65°-widefield OCTA (WF-OCTA) imaging device acquiring scans in less than 15 s and to compare it to ultrawidefield fluorescein angiography (UWF-FA).

⇒ Examination of OCTA B-scans for NV, visible as blood flow signals breaching the internal limiting membrane, revealed a sensitivity of 0.95 for PDR diagnosis. On UWF-FA, the majority of NV (63%) were located in the temporal quadrants with 93% of them being detected using single-capture WF-OCTA.

HOW THIS STUDY MIGHT AFFECT RESEARCH, PRACTICE OR POLICY

⇒ The high sensitivity of single-capture WF-OCTA in diagnosis of PDR in comparison to UWF-FA can improve clinical management of patients with diabetes. Quick and non-invasive single-capture 65°-WF-OCTA has the potential to replace UWF-FA as a single diagnostic tool.

INTRODUCTION

Proliferative diabetic retinopathy (PDR) with retinal neovascularisation (NV) affects nearly 7% of patients with diabetes.[1] Nearly half of those patients are at risk of developing retinal detachment and vitreous haemorrhage with severe vision loss if left untreated.[2] Therefore, the detection of diabetic NV is essential to diagnose PDR and offer adequate treatment. The modified Airlie-House-Classification from the Early Treatment Diabetic Retinopathy Study (ETDRS) was introduced three decades ago to determine stages of DR. Here seven stereoscopic pictures (seven standard fields) are used, which combined show approximately 34% of the retina to evaluate lesions.[3] With the development of ultrawidefield (UWF) imaging modalities offering a large field of view (FOV), allowing the detection of diabetic lesions in the periphery, stage of DR can be assessed quickly and with a high agreement to the seven standard fields of the modified Airlie House classification.[3–5] Fluorescein angiography (FA) is still the standard tool for assessing advanced stages of DR, including PDR by detecting retinal NVs. The combination of FA with UWF is time-efficient and reveals significantly more vascular pathology compared with the conventional seven standard

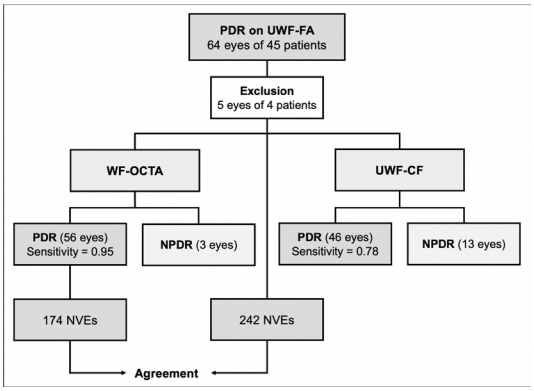

Figure 1 Flow chart of eyes with proliferative diabetic retinopathy (PDR) diagnosed using ultrawidefield fluorescein angiography (UWF-FA). Sensitivity of correct PDR diagnosis was evaluated with widefield optical coherence tomography angiography (WF-OCTA) and on ultrawidefield colour fundus (UWF-CF) images. 174 and 242 locations of neovascularisations elsewhere (NVE) were identified with WF-OCTA and UWF-FA, respectively. Agreement of NVE detection in total and each quadrant between WF-OCTA and UWF-FA was assessed.

fields.[6] Therefore, ultrawidefield-FA (UWF-FA) has been widely adapted as an easy and reliable way to confirm diagnosis of PDR. Although rare, adverse reactions can occur during or after FA.[7 8] Since its introduction, optical coherence tomography angiography (OCTA) has proven to be a non-invasive method offering high-resolution angiograms for evaluation of diabetic microvascular features including NV.[9–13] Furthermore, it has been shown that OCTA can improve clinical evaluation of DR by detecting small NV not seen during clinical examination or grading of the seven standard fields.[12]

This study aims to analyse the detection rate of single-capture wide-field (WF)-OCTA in comparison to UWF-FA and UWF-colour fundus (CF) in a clinical setting.

METHODS

The study was performed in accordance with the International Conference on Harmonisation of Technical Requirements for Registration of Pharmaceuticals for Human Use – Good Clinical Practice (ICH-GCP) guidelines.

Patients were recruited from the outpatient clinic of the unit for diabetic ocular diseases (figure 1) after routine clinical examination including visual acuity (in logMAR), slit-lamp examination, UWF-CF and UWF-FA (Optos, Dunfermline, Scotland, UK). When NV elsewhere (NVE)/(NV at the disc) (NVD) was detected on UWF-FA, patients were included in our study after informed consent was given.

UWF-CF images were analysed for diabetic NVs by two retinal experts.

A 65°-widefield-Swept-Source-OCTA (WF-SS-OCTA) was performed with a modified PlexElite system (Carl Zeiss Meditec, Dublin, California, USA) developed at the Center for Medical Physics and Biomedical Engineering at the Medical University of Vienna. The 2048 × 2 ×2048 A-scans were acquired with 1.680 MHz, a centre wavelength of 1060 nm, an axial resolution of 9 µm and a lateral resolution of 20 µm providing a 65° FOV with a diameter of 18 mm in a single-capture image (figure 2A). Acquisition time was less than 15 s. Angiograms were visually enhanced using a deep learning-based algorithm for denoising. Patients with severely reduced image quality due to media opacity or motion artefacts because of limited compliance were excluded from further analysis.

B-scans were assessed for supraretinal flow breaching the internal limiting membrane (ILM) and reaching into the posterior hyaloid as seen in figure 2B by two independent graders certified by the Vienna Reading Centre.

Detection of PDR was defined as visualisation of at least one NV inside the provided OCTA-FOV with flow breaching the

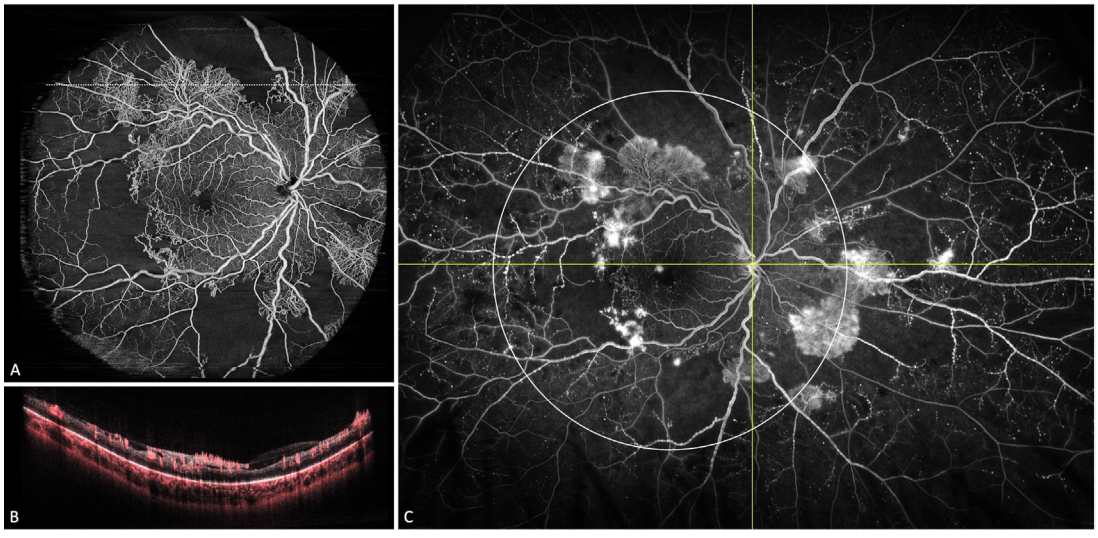

Figure 2 Patient presenting with acute vision loss of the left eye, due to vitreous haemorrhage. The treatment-naïve right eye presented with multiple neovascularisations (NV) as shown in A–C. (A) Single-capture wide-field optical coherence tomography angiography (WF-OCTA) with dashed line corresponding to the B-scan in B. (B) B-scan showing a disruption and flow above the internal limiting membrane representing diabetic NV. (C) Ultrawidefield fluorescein angiography (UWF-FA) (acquired at 1′31″) shows areas of NV as hyperfluorescent leakage. The white circle corresponds to the field of view seen with single-capture WF-OCTA. The yellow lines divide the UWF-FA image into four quadrants: superotemporal, inferotemporal, superonasal, inferonasal.

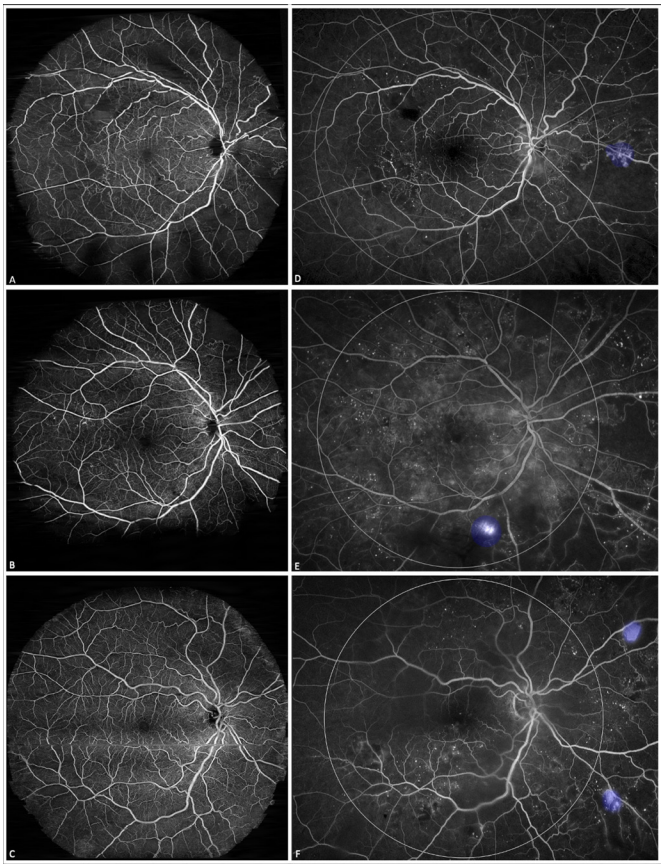

Figure 3 Three eyes with proliferative diabetic retinopathy. (A–C) Single-capture wide-field optical coherence tomography angiography (WF-OCTA) image showing various signs of diabetic retinopathy including multiple microaneurysms, non-perfusion areas (NPA) and intraretinal microvascular abnormalities (IRMA), but no neovascularisation (NV). (D) Ultrawidefield fluorescein angiography (UWF-FA) (acquired at 23″) with simulated single-capture WF-OCTA field of view (FOV) (white circle). The larger FOV of UWF-FA showed a neovascularisation (highlighted in blue) nasal to the optic disc slightly outside the WF-OCTA FOV. (E) UWF-FA (acquired at 1′16″) showing inferotemporal NV not visible on the corresponding WF-OCTA image (B) due to the loss of signal which resulted in a smaller FOV. (F) UWF-FA (acquired at 1′18″) showing two nasal NVs outside the WF-OCTA FOV.

ILM visible on the B-scan, which resulted in the correct assessment of DR-stage. Therefore, detection rate was the number of patients assessed correctly in comparison to UWF-FA.

The absolute number of NV detected in the UWF-FA FOV in total and in each quadrant (superotemporal, inferotemporal, superonasal and inferonasal as seen in figure 2C) was evaluated and compared with the number seen using WF-OCTA. This comparison was also made for an UWF-FA FOV reduced to the size of the WF-OCTA FOV to compare detection in the same area.

Furthermore, NV sites were examined in each eye and distinguished as NV at the disc (NVD), NV elsewhere (NVE), NVD/NVE only, and both NVD and NVE present on both devices. The distance of the NVE sites was measured in mm from the optic disc margins to the area of leakage in each quadrant on UWF-FA images using the Optos' built-in measurement tools.

According to the ETDRS report number 10, we defined intraretinal microvascular abnormalities (IRMAs) as tortuous vascular segments on CF images which were graded by two retinal experts certified by the Vienna Reading Centre.[3] Using UWF-FA, IRMAs were characterised as irregular flow lesions with no or minimal leakage.[14] With OCTA, IRMAs were previously described as irregular vasculature without breach of the ILM in the B-scan.[15]

OCTA- and FA-images were evaluated separately for the presence of IRMAs by two graders.

Statistical analysis

Qualitative variables are reported as absolute frequencies and percentages. Quantitative variables are summarised as mean±SD if not stated otherwise.

An estimate with 95% confidence limits of the sensitivity of PDR diagnosis using WF OCTA was derived from a GEE model with patient as repeated factor, to consider that some patients had measurements on both eyes.

Weighted kappa coefficients with 95% CIs were calculated for each area separately, using Fleiss Cohen weights. To compare the number of NVEs between the quadrants, a Friedman test was applied. The Holm method was applied to correct for multiplicity, adjusting for the number of areas. Distances of NVEs to the optic disc were compared between the quadrants using a mixed model (SAS Proc mixed). Significance level has been set to alpha=0.05.

RESULTS

Single-capture WF-OCTA was performed in 64 eyes of 45 with NVE detected on UWF-FA. 62% (n=28) were male and 38% (n=17) female. Mean visual acuity in logMAR was 0.17±0.23. 22 patients (49%) had type I and 23 patients (51%) type II diabetes with a mean diabetes duration of 19.8±12.5 years. Mean hemoglobin A1c (HbA1c) was 7.2±1.9% (n=38). For 7 patients HbA1c was unknown.

After 5 eyes (8%) of 4 patients were excluded due to reduced OCTA signal because of media opacity (n=2) and poor cooperation (n=3), 59 eyes (31 right eyes and 28 left eyes) of 41 patients were included in the final analysis. Thirty-three of those eyes (56%) were treated prior to study enrollment with panretinal photocoagulation (PRP).

On UWF-CF images, PDR was diagnosed in 46 eyes (sensitivity: 0.78, 95% CI 0.65 to 0.87), while on WF-OCTA scans 56 eyes were graded as PDR (sensitivity: 0.95, 95% CI 0.85 to 0.98).

With WF-OCTA, NVEs not depicted in four eyes lead to the diagnosis of NPDR in three eyes (shown in figure 3A–F) and one eye was graded as NVD only.

By evaluating every B-scan in our study population, we did not detect flow signals not corresponding to leakage seen on FA in our cohort.

On UWF-FA 93% of eyes had NVE of which 20% and 73% presented with and without NVD, respectively. 7% of eyes had NVD only. Of the total 242 NVEs seen on UWF-FA, 153 (63.2%) were located in the temporal and 89 (36.8%) in the nasal quadrants. With WF-OCTA we detected 92.8% (n=142) and 36% (n=32) of the NVEs seen on UWF-FA in the temporal and nasal quadrants, respectively. Although most NVEs were located inferotemporal (32%), followed by superotemporal (31%), inferonasal (19%) and superonasal (18%), there was no significant difference in the median number of NVEs between areas (Friedman test: p=0.1).

Agreement of NVE detection between UWF-FA and WF-OCTA was high in the temporal (superotemporal: κ=0.98, 95% CI 0.95 to 1; inferotemporal: κ=0.94, 95% CI 0.88 to 1) and weak in the nasal quadrants (superonasal: κ=0.24, 95% CI

Table 1 Sensitivity of WF-OCTA in comparison to UWF-FA in diagnosing PDR and agreement between devices in detecting NVE

	UWF-FA	WF-OCTA	
Diagnosis PDR, n of eyes (%)	59 (100%)	56 (95%)*	TPR=0.95 (95% CI 0.85 to 0.98)
Eyes with NVD	16 (27.1%)	16 (27.1%)*	
Eyes with NVD only	4 (6.8%)	5 (8.5%)*	
Eyes with NVE	55 (93.2%)	51 (86.4%)*	
Eyes with NVE only	43 (72.9%)	40 (67.8%)*	
Eyes with NVD and NVE	12 (20.3%)	11 (18.6%)*	
No of NVE seen on UWF-FA	242 (100%)	174 (71.9%)*	
No of NVE in quadrants			
Superotemporal	75 (30.9%)	71 (29.3%)*	
Inferotemporal	78 (32.2%)	71 (29.3%)*	
Superonasal	43 (17.7%)	14 (5.8%)*	
Inferonasal	46 (19%)	18 (7.4%)*	
Median n of NVE/eye			
In total (IQR)	3 (1–7)	2 (1–4)	κ=0.76 (95% CI 0.6 to 0.91)
Superotemporal	1 (0–2)	1 (0–2)	κ=0.98 (95% CI 0.95 to 1)
Inferotemporal	1 (0–2)	1 (0–2)	κ=0.94 (95% CI 0.88 to 1)
Superonasal	0 (0–1)	0 (0–0)	κ=0.24 (95%CI −0.04–0.5)
Inferonasal	0 (0–1)	0 (0–0)	κ=0.42 (95%CI 0.17 to 0.66)

Distribution of NVD and NVE in eyes on UWF-FA and WF-OCTA.
*Percentage of the total number of eyes or NVEs seen on UWF-FA.
NVD, neovascularisation at the disc; NVE, neovascularisation elsewhere; OCTA, optical coherence tomography angiography; PDR, proliferative diabetic retinopathy; TPR, true positive results; UWF-FA, ultrawidefield fluorescein angiography; WF-OCTA, widefield-OCTA.

−0.04 to 0.5; inferonasal: κ=0.42, 95% CI 0.17 to 0.66). Of the 242 NVEs (100%) seen on UWF-FA, 174 (71.9%) were visible on WF-OCTA. Of the 68 NVEs (28.1%) not seen on WF-OCTA, 63 were located outside the FOV (n=3 superotemporal, n=3 inferotemporal, n=29 superonasal and n=28 inferonasal). Details of NVE distribution are listed in table 1.

Comparing the same FOV on both devices we had an agreement over all areas of κ=0.99 (95% CI 0.98 to 1). In five eyes, we diagnosed one additional NVE with UWF-FA compared with WF-OCTA. Four NVEs were located inferotemporal and one superotemporal near the edges of the scan and were not visible due to reduced quality. In only one eye, a different stage of DR was assessed (figure 3B,E). Agreement in the superotemporal, inferotemporal, superonasal and inferonasal quadrant was κ=0.99 (95% CI 0.98 to 1), κ=0.96 (95% CI 0.93 to 1), κ=1 (95% CI 1 to 1) and κ=1 (95%CI 1 to 1), respectively.

Mean distance of NVE sites from optic disc margins was 6.7±2.3 mm with 7.1±1.9 mm, 7.6±2.1 mm, 5.7±2 mm and 5.3±2.3 mm in the superotemporal, inferotemporal, superonasal and inferonasal quadrant, respectively. There was a significant difference between areas (F-test: p<0.0001) with shorter distances in the nasal quadrants compared with the temporal quadrants. The mixed model revealed a statistically significant effect of prior PRP (estimate (95% CI) 1.0 (0.1 to 1.9), p=0.02) and disease duration on distance of NVEs (estimate (95% CI) 0.04 (0.003 to 0.08), p=0.04), with previous treatment and longer duration leading to farther distances. The effect of diabetes type (estimate (95% CI) 0.08 (–0.86 to 1.03), p=0.9) and HbA1c (estimate (95% CI) −0.1 (−0.4 to 0.2), p=0.5) was not statistically significant. No statistically significant effect of diabetes type, prior PRP, diabetes duration or HbA1c on the number of NVE was found (P values ranging from 0.1 to 1).

IRMAs were detected in 58 out of 59 eyes on UWF-CF images. In one eye (2%), no IRMAs were visible in a patient with NVD only and prior PRP. Using WF-OCTA and FA-images, IRMAs were detected in 57 (Sensitivity: 98%) and 55 eyes (SEnsitivity: 95%), respectively. IRMAs in one eye were missed with WF-OCTA due to reduced image quality at the edges of the scan. In three eyes, IRMAs were not detected with UWF-FA due to insufficient quality of the angiograms. The high resolution of the OCT angiograms led to a higher sensitivity of IRMA detection.

DISCUSSION

In our prospective, cross-sectional study, we evaluated the diagnostic value of WF-OCTA for detecting NVEs using a single-capture OCTA scan. To our knowledge, this is the first study to evaluate sensitivity of NV detection with WF-OCTA without the need montaging of several scans but using a 65° single-capture image.

We found that the sensitivity of WF-OCTA in detecting PDR was 0.95 (95% CI 0.85 to 0.98), improving non-invasive clinical diagnosis in comparison to UWF-CF photography, which showed a sensitivity of 0.78 (95% CI 0.65 to 0.87). Agreement of NVE detection in comparison to UWF-FA was high in the temporal and weak in the nasal quadrants. However, NVEs were more prevalent and located further from the disc in the temporal quadrants with 93% of them being detected on WF-OCTA scans.

OCTA has proven to be a reliable tool in assessing eyes in all stages of DR, whether for classification purposes or analysis of the retinal microvascular structure.

However, to be used as a single diagnosis tool, OCTA has to be directly compared with FA and new guidelines as to how to differentiate between active NV from quiescent NV or IRMA have to be adopted since visualisation of leakage is not an option. Since Tian *et al* described that IRMA were detected most frequently in the retinal slab and found no significant difference compared with the superficial slab for most diabetic features, we evaluated only the retinal slabs for NVs and IRMAs.[16]

Lee *et al* and Hwang *et al* were among the first to describe OCTA features of diabetic retinopathy showing a new approach of NV diagnosis not relying on leakage but identification of a vascular extension showing a flow signal breaching the ILM.[15 17] Lee *et al* further differed IRMAs from NVs by hyper-reflective dots in the superficial inner retina and an outpouching of the ILM without supraretinal flow.[15] This definition provides histopathologic insight and its reliability has since been confirmed by other authors.[14 18 19] In our study, we were also able to distinguish IRMAs from NVs by evaluating B-scans for a breach of the ILM which allowed an accurate differentiation, especially in patients with multiple small microvascular lesions as shown in figure 4. The high resolution of WF-OCTA led to a higher sensitivity of IRMA detection compared with UWF-FA and is in line with recent findings that OCTA allows a more detailed classification of IRMAs.[20]

You *et al* showed that in some patients who had been clinically graded as NPDR OCTA can reveal unsuspected NV and therefore improve non-invasive clinical evaluation in patients with different stages of DR.[12] Other studies have shown that by using composite images creating an FOV only slightly smaller than seen on UWF-FA, all NVs can be detected if not located outside the visible area.[21 22] Therefore, it is essential to acquire as much retinal area as possible, to provide the information needed for correct classification of DR stage.

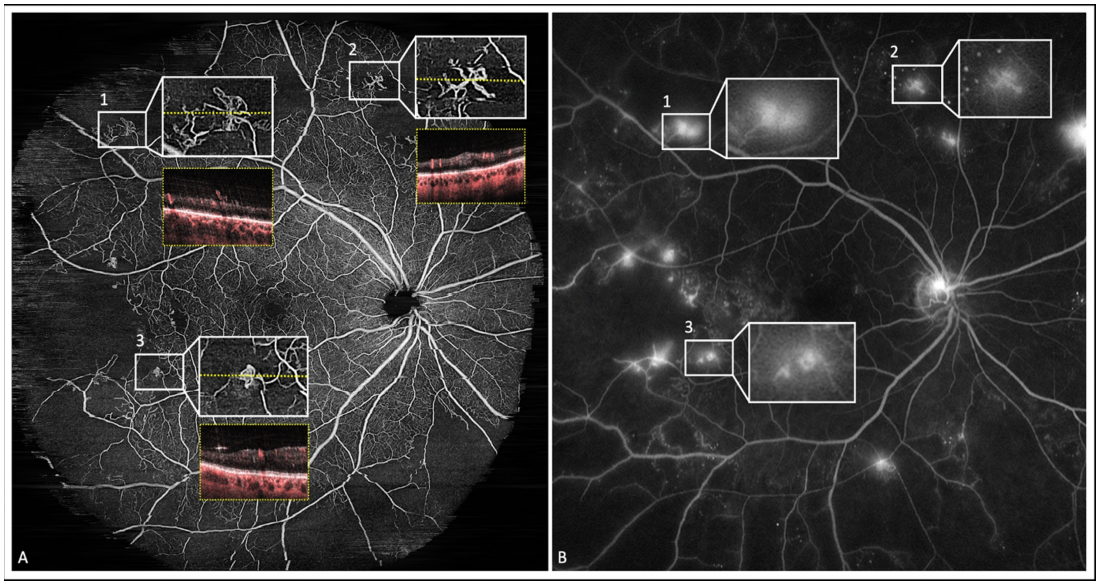

Figure 4 Patient presenting with treatment-naïve proliferative diabetic retinopathy. (A) Single-capture wide-field optical coherence tomography angiography (WF-OCTA) with three magnified microvascular lesions and dashed yellow line corresponding to the B-scans below. (A1) B-scan shows supraretinal flow signal breaching the internal limiting membrane (ILM), the main diagnostic criteria for diabetic neovascularisation (NV). (A2, A3) Two intraretinal microvascular abnormalities (IRMA) showing an outpouching of the ILM without supraretinal flow and can therefore be differentiated from NVs. (B) Corresponding ultrawidefield fluorescein angiography (UWF-FA) (acquired at 1'23") with the same magnified lesions as in A. (B1) NV shows diffuse hyperfluorescent leakage. (B2, B3) IRMAs show no real leakage in the late-phase UWF-FA. However, leakage of very small NV (B1) and hyperfluorescent vascular structure of IRMAs (B2, B3) are harder to distinguish using UWF-FA than evaluation of WF-OCTA images regarding flow breaching the ILM (A1).

In our study, evaluation of UWF-CF images showed a sensitivity of 0.78 in detecting PDR in comparison to 0.95 with WF-OCTA highlighting that WF-OCTA can improve clinical examination providing a fast and non-invasive approach. When comparing the same 65° area on both devices, we were able to diagnose PDR in 98% of eyes, with an almost perfect agreement of NVE detection in the temporal and a perfect agreement in the nasal quadrants.

Different approaches to acquire a larger FOV and therefore labelling the imaging method 'WF-OCTA' have been reported, whether with commercial or prototype devices. You *et al* achieved WF-OCTA images by montaging five 6×10 mm scans into a 25×10 mm acquired with a 200 kHz SS-OCTA prototype device using 1.4 mW light source at 1050 nm centre wavelength and three 6×6 mm scans from a 70 kHz commercial device with 840 nm central wavelength into a 15×6 mm image.[12] Cui *et al* created a 15×15 mm 50° FOV montage consisting of two 15×9 mm images using a commercial 100 kHz SS-OCTA with 1060 nm wavelength.[11] A frequently used method is the of 12×12 mm FOVs with five visual fixations to obtain an even larger FOV.[21–23] This FOV was evaluated by Russell *et al* in a different study to measure 22.1±3.64 x 21.6±3.42 mm.[24] Nevertheless, these large FOVs are harder to obtain requiring longer acquisition time and involving the risk of more artefacts. Cui *et al* used a motion artefact score as quality parameter to assess different DR stages and found that more severe stages had significantly higher motion artefact scores. Segmentation errors also occurred most frequently in the PDR group (50%) compared with the NPDR (10%) and the healthy group (0%). Lower BCVA and a longer scan time both contribute to a patients' fixation ability.[25] Therefore, shorter acquisition times ideally accomplished by a large FOV with a single-capture image are essential to enhance quality in WF-OCTA. Our prototype provides a 65° FOV (18 mm in diameter) in a single fovea-centred image acquired in less than 15 s. This allows good visualisation of the retina up to the mid periphery even in patients with fixation problems which is essential in advanced stages of DR for NV detection.

Taylor and Dobree first evaluated the distribution of NVs using retinal photographs describing that the most common sites of these NVs were the optic disc (25.4%) and the upper temporal vein (25.4%), followed by the lower temporal vein (19%), upper nasal vein (14.9%) and lower nasal vein (11.7%). Lesions only at the disc occurred in 16.3% corresponding to 5.6% of all sites. In addition, they found that lesions of the temporal venous branches occurred further from the disc than those of the nasal venous branches.[26] Russell *et al* described a similar distribution regarding temporal and nasal hemisphere with the highest prevalence of NVEs in the superotemporal quadrant in a large case series of 651 eyes of 433 patients using UWF-FA images. For treatment-naïve eyes, they reported 29.4%, 25.6%, 23.2% and 21.8% of NVEs in the superotemporal, inferotemporal, inferonasal and superonasal quadrant, respectively. In previously treated eyes, the corresponding percentages were 31.8%, 27%, 20.2% and 22.4%, respectively. Although in the nasal quadrants the higher prevalence changed from inferonasal to superonasal in the previously treated group, they reported no significant difference. Most patients had NVE only (48.4%), followed by NVE and NVD (41.8%), and NVD only (9.8%), without significant difference between treatment-naïve and previously treated eyes. After treatment, they noted no change of NV distribution.[24] Feman *et al* also reported that the superotemporal quadrant was the most frequent initial site.[27] In contrast to these results Jansson *et al* found that the majority of NVEs were located inferonasal to the optic disc and along the superior vascular arcades using a topography of merged retinal charts.[28]

Most NVEs were detected within the equator and the mean distance from the optic disc was between 5 and 6 mm with nasal lesions lying closer to the optic disc than temporal lesion.[26–28]

In our study, most eyes had NVE only (73%), followed by NVD and NVE (20%) and NVD only (7%). On UWF-FA images NVEs were most prevalent in the inferotemporal (32%) and superotemporal quadrants (31%), followed by the inferonasal (19%) and superonasal quadrants (18%). Our results are in line with previous findings, as the mean distance of NVEs from the optic disc was significantly shorter in the nasal quadrants in comparison to the temporal quadrants. The mean distance of all NVEs (6.7±2.3 mm) was slightly higher than previously reported. While we could not find a factor influencing the number of NVEs in each quadrant, we found that both disease duration and prior PRP lead to longer distances of NVEs from the optic disc.

Russell *et al* evaluated if the modern OCTA devices were able to detect most NVEs in eyes with PDR by overlaying a simulated 12×12 mm and montage WF-OCTA FOVs. At least one NV was visible in 83.9% of all eyes within the simulated 12×12 mm and in 98.3% within the simulated montage WF-OCTA FOV (22.1±3.64 × 21.6±3.42 mm). 37.2% and 80.3% of the total NV sites were detected in the simulated 12×12 mm and in the montage FOV, respectively.[24]

Our results are in line with these findings, showing single-capture WF-OCTA is able to detect at least one NVE in 95% of eyes leading to the correct diagnose of PDR. In the temporal quadrants, which showed the highest prevalence of diabetic proliferations, we observed an almost perfect agreement to UWF-FA by detecting 93% of all NVEs. Over all, we detected 72% of all NVEs visible on UWF-FA within our FOV.

Since in the temporal quadrants both prevalence and distances of NVEs from the optic disc was higher, a fovea-centred single-capture WF-OCTA scan is able to detect most NVEs. However, since distances of NVEs were shorter in the nasal quadrants (<6 mm), an additional, disc-centred scan could detect a majority of nasal proliferations with a total image acquisition time of less than 30 s.

A strength of this study is its prospective character and the single-capture WF-OCTA approach.

Although image acquisition is performed quickly and non-invasive, a limitation of WF-OCTA technology is the need to evaluate each B-scan manually by scrolling through the image volume for the diagnosis of NVs. Another limitation is the inconsistent quality at the edges of the OCTA scans reducing the FOV and potentially leading to NVEs undetected, which was the case in five eyes in our cohort. However, this resulted in a lower DR stage in only one eye.

In conclusion, our analysis showed that WF-OCTA improves non-invasive clinical diagnosis in diabetic patients by detecting NVs with a higher sensitivity than on UWF-CF images. Agreement of NVE detection in comparison to UWF-FA was high in the temporal and weak in the nasal quadrants. Distribution of NVEs showed a trend towards the temporal quadrants with most of them being detected on WF-OCTA. Nasal NVEs were located closer to the optic disc.

Due to its high reliability in detecting NVs, single-capture WF-SS-OCTA offers a quick and non-invasive alternative to UWF-FA for diagnosis and monitoring of PDR potentially replacing it in clinical routine for diabetic eye diseases when more widely available.

Contributors AP conceptualised the study and monitored data collection. He is guarantor. HS conceptualised the study, drafted the manuscript and prepared the figures. HS, JI and AS performed the image acquisition and image analyses. IS planned and performed the statistical analysis of the data. MN, ThS, WD, TiS and RL implemented the device used for this study. AP, MN, ThS, SS, WD, TiS, RL and UMS-E revised the manuscript.

Funding This work was supported by European Commisson H2020 programme initiated by the Photonics Public Private Partnership grant number MOON 732969.

Competing interests Research was funded by European Commisson H2020 programme initiated by the Photonics Public Private Partnership (MOON number 732969). UMS-E is a scientific consultant for Genentech, Heidelberg, Kodiak, Novartis, RetinSight, and Roche; and provides contract research for the Medical University of Vienna for Apellis, Genentech and Kodiak. SS is an advisory board member at Bayer, Roche and Novartis. AP is a scientific consultant for Bayer, Roche, Novartis and Oertli Instruments and received financial support by Roche. MN and ThS are consultants for Carl Zeiss Meditec. WD and RL are consultants for and received financial support by Carl Zeiss Meditec. TiS is an employee at Carl Zeiss Meditec Inc. The following athors have no financial disclosures: HS, JI, AS, IS.

Patient consent for publication Consent obtained directly from patient(s).

Ethics approval This study involves human participants and was approved by Medical University of Vienna ethics committee 1420/2018. Participants gave informed consent to participate in the study before taking part.

Provenance and peer review Not commissioned; externally peer reviewed.

Data availability statement Data are available on reasonable request. Unidentifiable data that underline the results reported in this article could be shared on reasonable request sent to the corresponding author.

ORCID iDs
Heiko Stino http://orcid.org/0000-0003-0233-359X
Johannes Iby http://orcid.org/0000-0002-3927-5832
Ursula Margarethe Schmidt-Erfurth http://orcid.org/0000-0002-7788-7311
Andreas Pollreisz http://orcid.org/0000-0003-3902-239X

REFERENCES

1 Yau JWY, Rogers SL, Kawasaki R, *et al*. Global prevalence and major risk factors of diabetic retinopathy. *Diabetes Care* 2012;35:556–64.
2 Preliminary report on effects of photocoagulation therapy. The diabetic retinopathy study research group. *Am J Ophthalmol* 1976;81:397–402.
3 Grading diabetic retinopathy from stereoscopic color fundus photographs--an extension of the modified Airlie house classification. ETDRS report number 10. Early treatment diabetic retinopathy study research group. *Ophthalmology* 1991;98:786–806.
4 Aiello LP, Odia I, Glassman AR, *et al*. Comparison of early treatment diabetic retinopathy study standard 7-field imaging with ultrawide-field imaging for determining severity of diabetic retinopathy. *JAMA Ophthalmol* 2019;137:65–73.
5 Silva PS, Cavallerano JD, Sun JK, *et al*. Nonmydriatic ultrawide field retinal imaging compared with dilated standard 7-field 35-mm photography and retinal specialist examination for evaluation of diabetic retinopathy. *Am J Ophthalmol* 2012;154:549–59.
6 Wessel MM, Aaker GD, Parlitsis G, *et al*. Ultra-wide-field angiography improves the detection and classification of diabetic retinopathy. *Retina* 2012;32:785–91.
7 Kwiterovich KA, Maguire MG, Murphy RP, *et al*. Frequency of adverse systemic reactions after fluorescein angiography. Results of a prospective study. *Ophthalmology* 1991;98:1139–42.
8 Yannuzzi LA, Rohrer KT, Tindel LJ, *et al*. Fluorescein angiography complication survey. *Ophthalmology* 1986;93:611–7.
9 Schaal KB, Munk MR, Wyssmueller I, *et al*. Vascular abnormalities in diabetic retinopathy assessed with swept-source optical coherence tomography angiography widefield imaging. *Retina* 2019;39:79–87.
10 Bradley PD, Sim DA, Keane PA, *et al*. The evaluation of diabetic macular ischemia using optical coherence tomography angiography. *Invest Ophthalmol Vis Sci* 2016;57:626–31.
11 Cui Y, Zhu Y, Wang JC, *et al*. Comparison of widefield swept-source optical coherence tomography angiography with ultra-widefield colour fundus photography and fluorescein angiography for detection of lesions in diabetic retinopathy. *Br J Ophthalmol* 2021;105:577–81.
12 You QS, Guo Y, Wang J, *et al*. Detection of clinically unsuspected retinal neovascularization with wide-field optical coherence tomography angiography. *Retina* 2020;40:891–7.

13 Soares M, Neves C, Marques IP, *et al*. Comparison of diabetic retinopathy classification using fluorescein angiography and optical coherence tomography angiography. *Br J Ophthalmol* 2017;101:62–8.
14 Arya M, Sorour O, Chaudhri J, *et al*. Distinguishing intraretinal microvascular abnormalities from retinal neovascularization using optical coherence tomography angiography. *Retina* 2020;40:1686–95.
15 Lee CS, Lee AY, Sim DA, *et al*. Reevaluating the definition of intraretinal microvascular abnormalities and neovascularization elsewhere in diabetic retinopathy using optical coherence tomography and fluorescein angiography. *Am J Ophthalmol* 2015;159:101–10.
16 Tian M, Wolf S, Munk MR, *et al*. Evaluation of different Swept'Source optical coherence tomography angiography (SS-OCTA) slabs for the detection of features of diabetic retinopathy. *Acta Ophthalmol* 2020;98:e416–20.
17 Hwang TS, Jia Y, Gao SS, *et al*. Optical coherence tomography angiography features of diabetic retinopathy. *Retina* 2015;35:2371–6.
18 DaCosta J, Bhatia D, Crothers O, *et al*. Utilisation of optical coherence tomography and optical coherence tomography angiography to assess retinal neovascularisation in diabetic retinopathy. *Eye* 2022;36:827–34.
19 Vaz-Pereira S, Silva JJ, Freund KB, *et al*. Optical coherence tomography angiography features of neovascularization in proliferative diabetic retinopathy. *Clin Ophthalmol* 2020;14:3351–62.
20 Shimouchi A, Ishibazawa A, Ishiko S, *et al*. A proposed classification of intraretinal microvascular abnormalities in diabetic retinopathy following panretinal photocoagulation. *Invest Ophthalmol Vis Sci* 2020;61:34.
21 Sawada O, Ichiyama Y, Obata S, *et al*. Comparison between wide-angle OCT angiography and ultra-wide field fluorescein angiography for detecting non-perfusion areas and retinal neovascularization in eyes with diabetic retinopathy. *Graefes Arch Clin Exp Ophthalmol* 2018;256:1275–80.
22 Pichi F, Smith SD, Abboud EB, *et al*. Wide-field optical coherence tomography angiography for the detection of proliferative diabetic retinopathy. *Graefes Arch Clin Exp Ophthalmol* 2020;258:1901–9.
23 Russell JF, Shi Y, Hinkle JW, *et al*. Longitudinal wide-field Swept-Source OCT angiography of neovascularization in proliferative diabetic retinopathy after panretinal photocoagulation. *Ophthalmol Retina* 2019;3:350–61.
24 Russell JF, Flynn HW, Sridhar J, *et al*. Distribution of diabetic neovascularization on ultra-widefield fluorescein angiography and on simulated widefield OCT angiography. *Am J Ophthalmol* 2019;207:110–20.
25 Cui Y, Zhu Y, Wang JC, *et al*. Imaging artifacts and segmentation errors with wide-field swept-source optical coherence tomography angiography in diabetic retinopathy. *Transl Vis Sci Technol* 2019;8:18.
26 Taylor E, Dobree JH. Proliferative diabetic retinopathy. Site and size of initial lesions. *Br J Ophthalmol* 1970;54:11–18.
27 Feman SS, Leonard-Martin TC, Semchyshyn TM. The topographic distribution of the first sites of diabetic retinal neovascularization. *Am J Ophthalmol* 1998;125:704–6.
28 Jansson RW, Frøystein T, Krohn J. Topographical distribution of retinal and optic disc neovascularization in early stages of proliferative diabetic retinopathy. *Invest Ophthalmol Vis Sci* 2012;53:8246–52.